Image analysis determination of particle size distribution

Maud Langton and Anne-Marie Hermansson

SIK-The Swedish Institute for Food Research, PO Box 5401, S-402 29 Göteborg, Sweden

Abstract. Three different methods for the determination of particle sizes by means of light microscopy combined with image analysis have been evaluated for dispersions of spherical starch particles. (i) Individual particles. This method was used to separate particles that formed clusters into individual particles. The size of the particles was determined by the diameters of the circles which could be inscribed in the cluster. (ii) Clusters. This method was used to measure all the connecting particles as one object, regardless of whether they were separated or in clusters. The area of the clusters was measured and the diameter of an equivalent circle was calculated. (iii) Strings of beads. This is a special case of clusters where particles were associated in one direction and formed strings. The diameter was the maximum distance between two parallel lines touching the object. Statistical evaluation of the results showed that there was very little variance between slides, frames and samples from the same batch. Thus repeated measurements with the image analysis system appear to be accurate. For the three image analysis methods the mean values of the particle size were between one micron to three microns.

Introduction

Accurate characterization of the particle size distributions in dispersions as well as in solid materials is important in the determination of the physical properties of a material. Several techniques can be used in order to determine particle size distribution, e.g. light scattering, microscopy, sieving, sedimentation analysis, permeability of a powder column and electrical-sensing zone technique. Different techniques measure different parameters; each technique has its advantages and disadvantages which have been discussed by Lammers *et al.* (1). The choice of technique would therefore largely depend on the application.

When a new technique is developed, such as image analysis, it is often compared with traditional techniques. The determination of the particle size distribution by image analysis exclusively has only been used when no other technique has been available, e.g. inclusions in steel (2). Microscopy combined with image analysis have previously been compared with light diffraction. There was fairly good agreement between the methods (3–7). Both light scattering, and microscopy with image analysis can be divided into several approaches and techniques. The difficulties of obtaining a true size distribution are associated with the parameters which are measured and calculated, and the assumptions that have to be made for the evaluation of the size distributions. Droplet sizes in emulsions has been determined by using a computerized imaging system and light scattering (7). The results showed that the light scattering method was appropriate for emulsions with average droplet diameters of <7.0 μm.

All measurements in the above mentioned comparative studies were made on particles of well-defined materials, such as carbonyl–iron powder, protein stabilized peanut oil-in-water emulsion, rubber and latex where the internal structure is known, e.g. the optical properties are measured yielding a value of

refractive index, etc. to enable accurate values for the light scattering method to be obtained. In these investigations the particles ranging from 0 to 20 μm were spherical and had no contact with each other, but in many cases the particles are clustered and are non-spherical.

The determination of larger particle size distributions, of non-agglomerated milk powders ranging from 10 to 130 μm has been done by Lammers *et al.* (1). They compared the results of measurements obtained from microscopy, Coulter counting and light diffraction with a Malvern particle sizer. In many cases the different techniques yield different results because the apparatus sense different phenomena. The Coulter counter senses net particle volume, the Malvern particle sizer senses projected area and the microscope measures something in between the largest and the average diameter of the diameter of each particle. Jokela *et al.* (6) pointed out that image analysis had certain advantages over the more established techniques, e.g. it can analyze non-conducting samples, unlike the Coulter counting method, and can discriminate between coalesced, flocculated and individual emulsion droplets, which cannot be done with the alternative techniques used in their study.

The aim of this study is to evaluate different approaches for determining size distribution by using image analysis combined with light microscopy. Three different approaches have thus been used: The first approach is used to separate the particles that form clusters in order to measure them individually. The second approach is used to analyze all objects whatever their shape as if they were circular particles. The third approach is used to analyze a special case of clusters, asymmetric clusters, when the particles are associated in one direction and form strings of beads. In this case the cluster size can be determined as the largest distance within the object. The different approaches were used to determine whether the particles formed clusters, and if so, whether they were oriented. The material used was a dispersion of spherical starch particles.

Material and methods

Material

Starch particles were produced by Biogram AB, Malmö, Sweden, 'Biogram Microspheres'. The particles contained ~25% starch. The process produced suspensions of spherical particles from 1 to 100 μm as estimated by light scattering. The instrument used was a Malvern Mastersizer, Malvern Instruments Ltd, Malvern, UK.

Light microscopy

The particle suspension was placed on a slide which was covered and sealed with entellan. The internal distribution between the particles may be rearranged, contrary to the sectioning technique where the internal distribution is maintained, but instead the particles are sectioned. In the case of sectioning one has to take into account how the section cuts through the particles. The spherical shape was confirmed by light microscopy, Microphot-Fx, Nikon Corp., Tokyo

Japan. Good contrast was obtained with iodine staining. The contrast was enhanced by a green interference filter, GIF, Nikon Corp., Tokyo, Japan. The difficulty of obtaining a good image of the emulsion droplets from the light microscope to the image analysis system is well described by Jokela *et al.* (6). The sample used here was very thin and the condenser aperture was set to give maximum contrast (~0.2) and no cut in the distribution could be observed.

The samples were examined under different magnifications with 10×, 20×, 40× objectives. Measuring at 10× did not result in finding larger particles than measuring at 20×, as one pixel corresponded to 0.9 microns, which gave a large cut in the distribution since many particles had a diameter of one micron.

Image analysis

An image processing system included the input units, host computer with image processors, and output units. The image analysis system used here was a Contextvision microGOP, from Struers Vision AB, Linköping, Sweden. Direct reading from the light microscope via the CCD-camera was also used. The CCD-camera has a resolution of 512 × 512 pixels with a depth of 256 grey levels.

The grey scale image had to be 'threshed' into a black and white, binary image. All measurements were obtained in the binary image. The pixel-scale values were converted into microns by a scaling factor which had been calibrated for each magnification (see Table I). The high contrast in the image made it possible easily to thresh the image into a binary image. Considering the fact that we were imaging whole particles, the binary image was manifested as a shadow of the outer edges of the particle. The particle size distribution was reduced when the frame-edge cut the particles. To reduce frame-edge effects, a measuring frame was laid on each image (full frame). The measuring frame was placed at 93 pixels from each side of the full frame (see Table I). The particles on the north and on the west side of the edge of the measuring frame were included in the measurements and particles hitting the east and south side were excluded from the measurements.

The output units of the system consisted of a Polaroid hard copy (photo of the screen), an Apple laser writer, a tape station and an optical disk station. The output data can be an image, data lists, calculated values, etc. Measured values on data lists are transferred from the internal GOP format, i.e. a floating point format, to ASCII text and transferred via the network to an IBM-PC for further evaluation.

Table I. Scale and size of the images

Magnification	Scaling factor (microns/pixel)	Full frame size (micron × micron)	Measure frame (micron × micron)
10×	0.8638986	440 × 440	280 × 280
20×	0.4282410	220 × 220	140 × 140
40×	0.2145143	110 × 110	70 × 70
80×	0.1072570	55 × 55	35 × 35

13

Sampling design and statistics

The difficulties connected with sampling have previously been pointed out (1). The dispersions were received in small glass tubes, from Biogram, Malmö, Sweden. The dispersion in one glass tube, a batch, was made with a specific set of production parameters. Two batches denoted batches I and II were examined. The small glass tubes were shaken and a part was taken from each batch, diluted with distilled water, vigorously mixed, stained with iodine, placed on slides, and covered and sealed. From one batch, two diluted sample solutions were measured and from each sample several slides were made of which two were measured. The slide to be measured was divided into nine squares. In each square one image was taken and transferred to the image analysis system. Three magnifications were used, 20×, 40× and 80× on the same slide (see Figure 1). On each slide a latin square sampling design was used, where A, B, C were randomly assigned to the magnification 20×, 40×, 80×, as illustrated in Figure 1. For each row and each column all three magnifications were used once. The image taken in each square was marked with the magnification used and with a letter connected with the geographic orientation on the slide. This was used to guard against the possibility of the dispersion spreading out unevenly on the slide, with large particles in the centre and the small ones towards the edges. For each column the three magnifications were merged to form one set of data. The high magnification, 80×, was used to detect small particles of <0.70 μm. Whereas 40× detected particles of between 0.70 and 2.40 μm, and 20× particles >2.40 μm. Twenty-five per cent of the data from one measuring frame at magnification 20× was randomly selected in order to obtain the same measurement area for both 40× and 20× magnifications. This procedure enabled variations within the same slide, between slides, samples and batches to be obtained.

The statistical calculation was made by means of the SAS-Statistical Analysis System, (8,9). The variance component model was estimated by means of PROC NESTED and the descriptive statistics by means of PROC UNIVARIATE.

Aa	Bb	Cc
Bd	Ce	Af
Cg	Ah	Bi

Fig. 1. Plan of geographic orientation and for choice of magnification, where A, B, and C = 20×, 40× and 80× are randomly drawn for each slide. a, b, c, d, e, f, g, h and i are the geographic orientations which are kept constant on all slides and a is always in the north-west corner.

14

Results

Image analysis

The first approach was to assume that all particles are individual and that no clusters exist. The agglomerate of particles in the image had to be separated; this was done by measuring the individual spheres. The particles touching each other were regarded as collisions.

By using a special software package for the microGOP devised by Struers Vision AB, Linköping, Sweden and ourselves, we were able to find the largest circles which could be inscribed in a hole or object. The program finds the
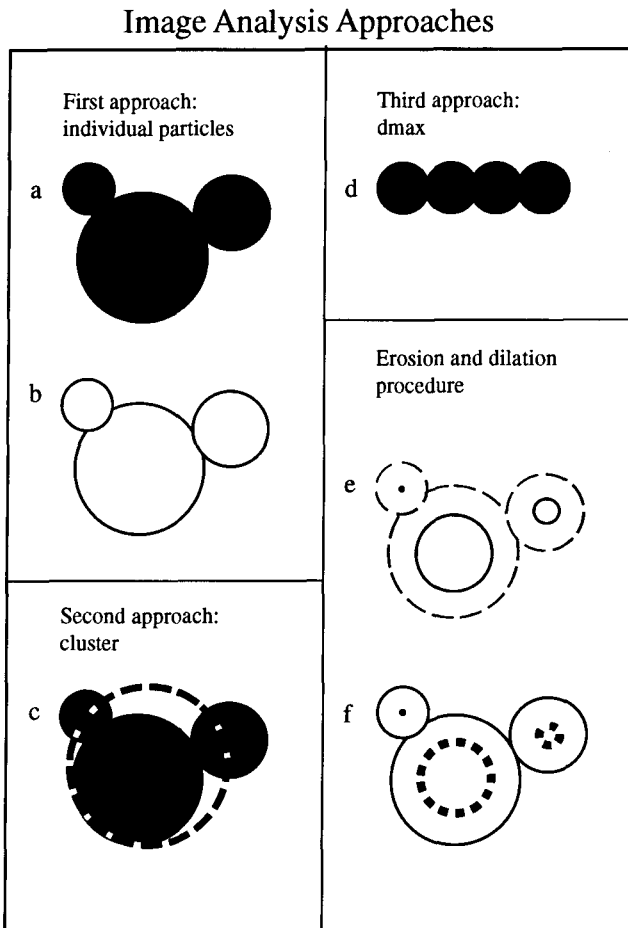
Image Analysis Approaches

Fig. 2. Schematic illustration of four image analysis approaches. a. The first approach showing a picture of a cluster and b. the circles which can be inscribed in it. c. The second approach showing a schematic drawing of a cluster with the D_{ec} marked by a broken circle. d. The third approach showing a drawing of particles that join in one end to form a string of beads. e. Another approach is shown by a schematic drawing of the original object with broken lines, and after the erosion steps drawn with solid lines. f. Dilation growing back towards the original dimensions.
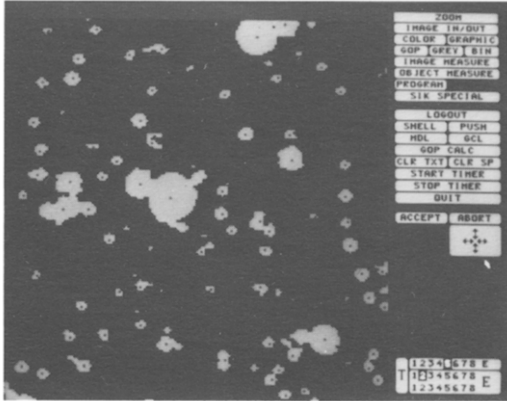
15

Fig. 3. An enlarged part of a binary image with the centres of the circles which can be inscribed marked by dots.

centres of circles (or the local maximum distance from the outer edge) and the diameter of the circle which can be inscribed in the hole or object. Figure 2a shows a schematic drawing of the object, a cluster of three particles and Figure 2b shows the three circles which fit in the object. Figure 3 shows a highly enlarged part of a binary image of the sample where the centres of the circles have been marked as dots. This creates the narrowest distribution with the smallest mean diameter of the particles. Figures 4 and 5 show the size distribution when the first approach is used on batches I and II respectively. The two batches had size distributions with a peak value of between one and two microns. No values were >20 microns. Most of the particles were small resulting in a large peak at low values and a long tail towards larger values. All particles, independent of sample, slide and column were included in the size distributions presented in Figure 4 and 5.

The second approach can be used when clusters exist. This approach is an averaging approximation and is commonly used to calculate the equivalent diameter of a circle when the area is measured. This gives an equivalent circle diameter of the cluster but does not differentiate between clusters and single particles. The approach is used to measure the total area from which the diameter is calculated. The function for calculating the diameter of an equivalent circle that would fit the measured area also exists in the standard software package. The diameter of equivalent circle D_{ec} is calculated as:

$$D_{ec} = 2\sqrt{(A/\pi)} \tag{1}$$

where A is the measured area of the object.

Figure 2c shows a cluster of three particles; D_{ec} is illustrated by the broken line. This gives an equivalent circle diameter of the cluster size. This distribution has a larger mean value than the previous measurement approach. The shape of the distribution curves for the cluster approach is the same as for individual particles; this was the case for all approaches. Figures 6 and 7 show size
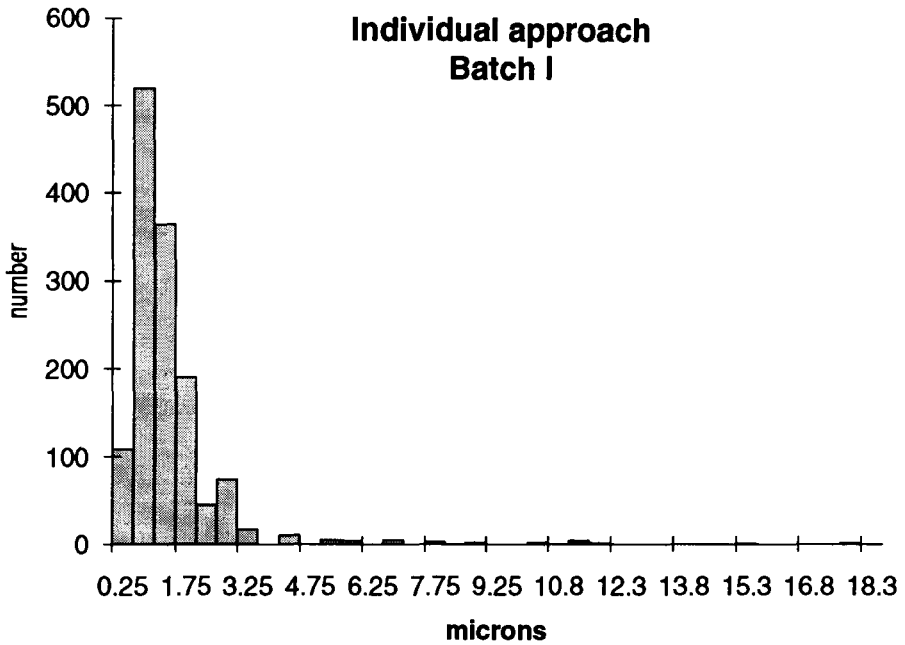
Fig. 4. Size distribution in microns by means of the individual approach used on batch I including all particles.
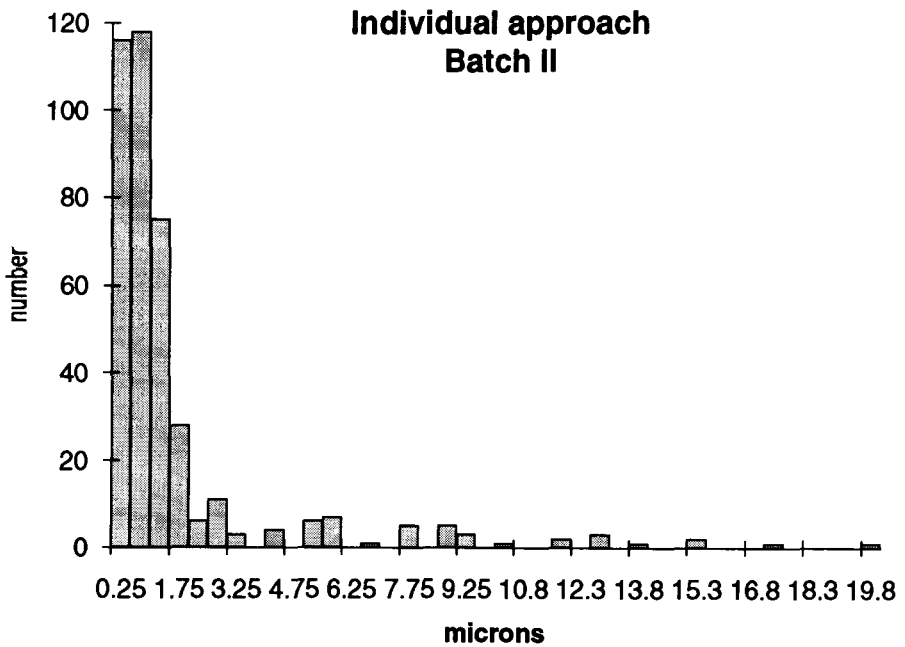

Fig. 5. Size distribution in microns by means of the individual approach used on batch II including all particles.
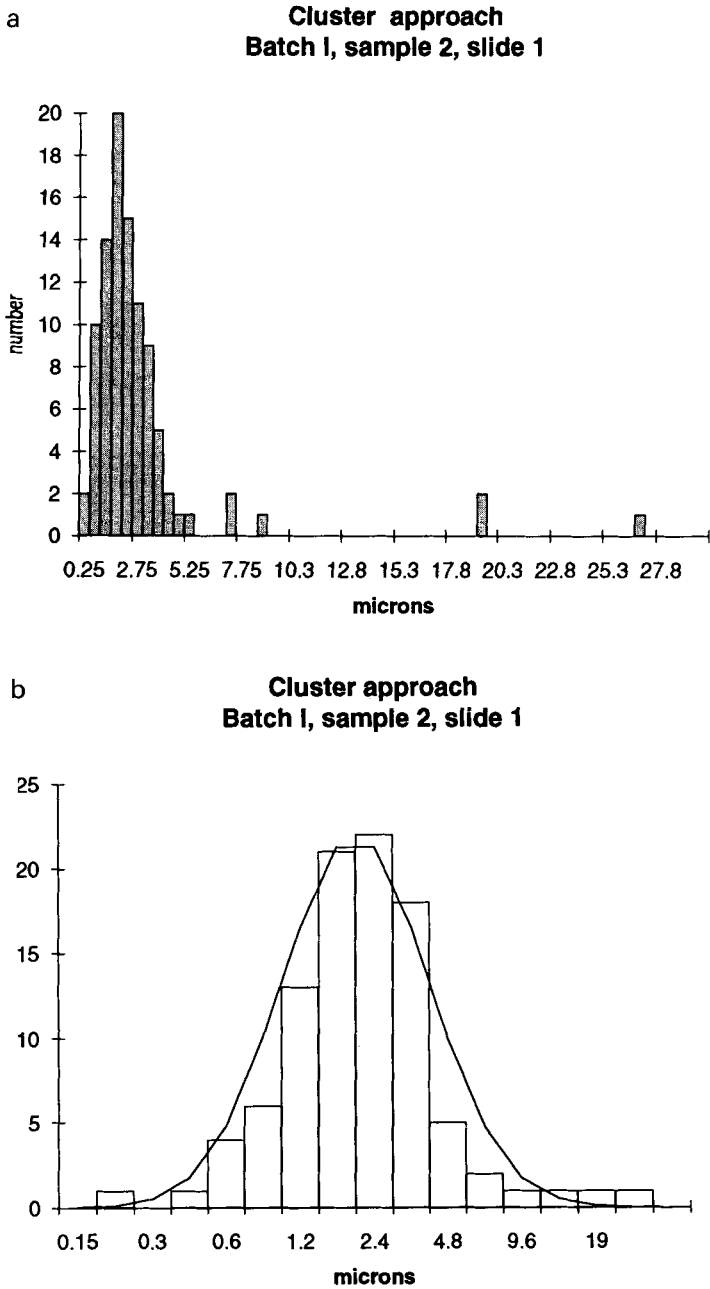
a
Cluster approach
Batch I, sample 2, slide 1

b
Cluster approach
Batch I, sample 2, slide 1

Fig. 6. Size distribution in microns by means of the cluster approach on batch I, one slide of sample 2; a, normal and b, log-normal.

18

a

**cluster approach
Batch I, sample 3, slide1**

b

**Cluster approach
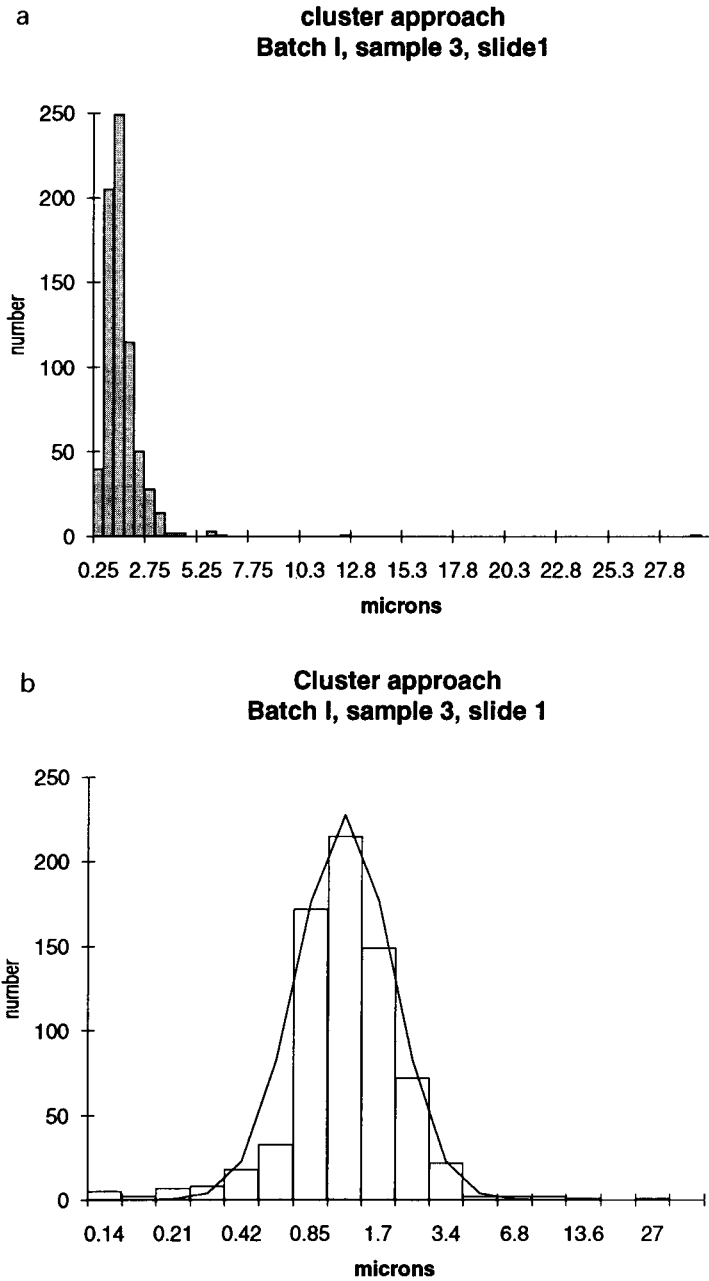Batch I, sample 3, slide 1**

Fig. 7. Size distribution in microns by means of the cluster approach on batch I, one slide of sample 3; a, normal and b, log-normal.

19

distributions of batch I for the cluster approach. Figures 6 and 7 show two different dilutions of batch I, a slide of sample 2 and sample 3 respectively. Sample 2 has fewer particles than sample 3, but is comparable in size. Figures 6a and 7a show the size distribution in count frequency in original scale, and Figures 6b and 7b show the same distribution in log scale. Figures 6b and 7b show that the size distributions are approximately log-normal for batch I using the cluster approach. Log-normality appears to be a reasonable approximation for these kinds of data irrespective of approach, batch, sample and slide. By using sieving Audet and Lacroix (10) also found log-normal size distributions for gel beads produced by means of the two-phase dispersion process. Log-normal size distributions are also common for many minced materials.

The third approach was used to find the largest dimensions of the objects. The largest dimension is especially important when the clusters are asymmetrical, i.e. when particles associate in one direction forming strings. If the associations between the spherical particles are strong the cluster is shaped like a rod instead of the assumed circle. The parameter $d$max for each object in a binary image is measured. Dmax is the maximum distance between two parallel lines touching the object. Figure 2b shows four particles associated in one direction and forming a string of beads.

The particle size can be described by the mean values of the distribution. Table II summarizes the mean values of the three approaches, individual, cluster and $d$max. The largest mean values, 2.4 and 2.2 μm, were obtained with the $d$max approach for batches I and II respectively. For batch I the individual approach yielded a lower mean value (1.4 μm) than for the cluster approach (1.9 μm), whereas for batch II the individual and the cluster approaches gave mean values of the same order, 1.7 μm. It seems that when particles cluster, the composition is one large particle with small ones attached to it.

A variance component model for log (diameter) in a nested model was used to analyze the results (11). In the variance component model batch, sample, slide and column were explanatory variables and the log size of the particle was the dependent variable. Column was nested within slide, slide was nested within sample and sample was nested within batch. Table III shows the estimates which were obtained. Note that the variation between particles had the largest effects and that the effect of sample, slide and column on the variation were small. Thus further measurements of these dispersions could be concentrated on particle-to-particle variations and batch effects, whereas sample, slide and column could be ignored.

To describe the width of the distribution, the 0.1 and 0.9 fractiles are often used together with the 0.5 fractile, P_{50}, which is the median value, and 90% of

Table II. Particle size (mean values in microns)

	Individual particles	Cluster $(D_{cc} = 2\sqrt{(A/\pi)})$	Dmax
Batch I	1.39	1.89	2.41
Batch II	1.72	1.69	2.24

the measured particles are finer than the 0.9 fractile value. These values become important when the desired distribution should be narrow towards a target median particle size. The median values of the three approaches for both batches followed the assumed order: P_{50} (individual) < P_{50} (cluster) < P_{50} ($d$max) and were lower than respective mean values. The fractiles are summarized in Table IV. Ninety percent of all particles were <4.3 μm independent of batch and approach.

Another approach for individual particles is to separate the particles by erosion and dilation steps. Particle separation is done by first shrinking, i.e. erosion of the particles, pixel by pixel, in eight directions. The effect of erosion is illustrated by Figure 2e. After this step the particles are restored to their original sizes by letting them grow, i.e. dilation, to the same number of pixels but without letting them grow together (see Figure 2) and then to calculate the diameter using the same method as in the cluster approach. This is a commonly used approach when a clear separation between particles does not occur (2,12). This approach has not been investigated in this study. If two particles are in contact with each other the first approach would give two diameters and the second approach one diameter of an 'average' particle, whilst the third approach would yield the largest distance in the cluster. The first individual particles approach and the erosion–dilation procedure should thus give similar results.

Discussion

In this study image analysis has been used to determine the size distributions. Light diffraction is a commonly used and rapid method for size-determination of particles. When light diffraction results are compared with image analysis results

Table III. Variance component model for log-diameter

		Percent of total
σ^2_{batch}	0	0
σ^2_{sample}	0.020	13.5
σ^2_{slide}	0.025	17.4
σ^2_{column}	0.012	8.3
$\sigma^2_{particle}$	0.089	60.8

Table IV. Size distribution in microns of batches I and II by means of different image analysis approaches

Batch	Fractile	Individual	Cluster	Dmax
Batch I	P_{10}	0.64	0.73	0.89
	P_{50}	1.28	1.51	1.78
	P_{90}	2.15	3.06	4.34
Batch II	P_{10}	0.21	0.17	0.21
	P_{50}	0.85	1.00	1.28
	P_{90}	4.28	3.14	3.88

Fractile P_{10} gives the size at which 10% of the particles is below the given value. Thus, the P_{50} is the median.

one has to keep in mind that the distribution functions are different. The light diffraction techniques are volume-sensitive and size distribution is given in parts of volume. In this study, image analysis results have been given in number distributions, although measurements can also be made in parts of area. A volume distribution is more sensitive to large particles, thus a couple of large particles can alter the whole distribution. However in a number distribution many small particles dominate and the mean value is usually smaller than for a volume distribution. For different measuring techniques to be compared one of the distributions has to be transformed to produce the same type of representation of the distribution. How the size-distribution is measured and presented, and in what way this is relevant for specific applications, must be considered. In some food applications the majority of many small particles have a large impact on physical and sensory properties, whereas a few large particles might be of importance for other applications.

An advantage of the image analysis technique is that it enables the determination of the size-distribution for particles of an unknown structure and of particles as inclusions. Image analysis results can also give some indication as to which value to chose for light diffraction measurements of a new material among parameters related to the optical properties. Image analysis can also be used to determine the effect of clustering on size-distribution. In this study clusters did not greatly affect the median value. The image analysis technique can be an important tool for size and coalescence or flocculation determinations, especially when dilution is not possible.

Acknowledgements

References

1. Lammers,W.L., van der Stege,H.J. and Walstra,P. (1987) *Netherlands Milk and Dairy Journal*, **41**, 147–160.
2. Rinaldi,F. and Rossi,M.A. (1987) *Metallography*, **20**, 385–400.
3. Hall,R.A., Hites,R.D. and Plantz,P. (1982) *J. Appl. Polym. Sci.*, **27**, 2885–2890.
4. Hall,R.A. (1988) *J. Appl. Polym. Sci.*, **36**, 1151–1155.
5. Japka.J.E. (1988) *J. Metals*, **40**, 18–21.
6. Jokela,P., Fletcher,P.D.I., Aveyard,R. and Lu,J.-R. (1990) *J. Coll. Interf. Sci.*, **134**, 417–426.
7. Klemaszewski,J.L., Haque,Z. and Kinsella,J.E. (1989) *J. Food Sci.*, **54**, 440–445.
8. *SAS/STAT User's Guide* (1990), Version 6, 4th Edn, **1**, SAS Institute Inc., Cary, NC, USA.
9. *SAS/STAT User's Guide* (1990), Version 6, 4th Edn, **2**, SAS Institute Inc., Cary, NC, USA.
10. Audet,P. and Lacroix,C. (1989) *Proc. Biochem.*, **14**, 217–226.
11. Nester,J., Wasserman,W. and Kutner,M.H. (1985) *Applied Linear Statistical Models*, Richard D Irwin Inc.
12. Farrants,G., Schuler,B., Karlsen,J., Reith,A. and Landgård,S. (1989) *Amer. Ind. Hyg. Assoc. J.*, **50**, 473–479.